IL NUOVO CIMENTO **38 C** (2015) 171
DOI 10.1393/ncc/i2015-15171-5

Colloquia: VILASIFEST

Geometric phase and its applications to fundamental physics

A. Capolupo and G. Vitiello

Dipartimento di Fisica E.R.Caianiello and INFN Gruppo collegato di Salerno, Università di Salerno, Fisciano (SA) - 84084, Italy

received 11 January 2016

Summary. — We report on recent results showing that the geometric phase can be used as a tool in the analysis of many different physical systems, as mixed boson systems, CPT and CP violations, Unruh effects, and thermal states. We show that the geometric phases appearing in the time evolution of mixed meson systems like B_s^0-$\bar{B}_s^0$ and the K^0-$\bar{K}^0$ are linked to the parameter z describing the CPT violation. A non-zero phase difference between particle and antiparticle arises only in the presence of CPT symmetry breaking. Then the geometric phase can represent a completely new test for the CPT invariance. Moreover, we study the geometric phase of systems represented by mixed state and undergoing a nonunitary evolution and propose the realization of interferometers which can prove the existence of the Unruh effect and can allow very precise measurements of temperature.

PACS 03.65.Vf – Phases: geometric; dynamic or topological.
PACS 11.10.-z – Field theory.
PACS 04.62.+v – Quantum fields in curved spacetime.

1. – Introduction

In the recent years, many studies have been devoted to the analysis of the geometric phase [1-24]. It characterizes the evolution of many physical systems and has been detected in different ways [25-29].

On the other hand, it has been shown [30,31] that in all the systems where the vacuum condensates are generated [32-40], the Aharonov-Anandan invariant [4] (AAI) and the geometric phase are produced in their evolution. This fact has suggested that phenomena like Unruh [36], Hawking [37] and Parker effects [38,39], characterized by the presence of a vacuum condensate and very hard to be detected, togheter with some aspect of quantum field theory in curved space, could be analyzed by means of the geometric phase of atomic systems which simulate such phenomena [30, 31]. It has been shown also that geometric phases and invariants can be used to test CPT symmetry in meson systems like kaons and B_s^0-$\bar{B}_s^0$ system [41], to prove the existence of postulated particles like the axions [42], to test SUSY violation in thermal states [43], to reveal the Hawking [30] and Unruh [30, 31, 45, 44] effect and to build a quantum thermometer [30, 31, 46].

In the present paper, we report the results obtained by studying the geometric phase for mixed meson systems [41] and for quantum open systems represented by atoms accelerated in an electromagnetic field and interacting with thermal states [31]. We reveal the relation between the geometric phase appearing in the evolution of mixed mesons and the parameter denoting the CPT violation [41]. We show that a non-trivial phase difference between particle and antiparticle indicates unequivocally the CPT symmetry breaking in mixed bosons. We also show that the phases can be useful for the study of the CP violation and we do a numerical analysis for B_s^0-$\bar{B}_s^0$ mesons [41].

We then study the geometric phase for quantum open systems [16] and we show that a detectable difference of the geometric phases can be revealed between atoms which are accelerated in an arm of an interferometer and atoms which are inertial in the other branch. Such a phase difference is due only to the Unruh effect [30, 31]. Moreover, we show that the difference between geometric phases produced by atoms interacting with two different thermal states allows to determine the temperature of a sample once the temperature of the other one is known [30, 31].

The use of the phase defined in [16] allows to consider time intervals arbitrary small and very low transition frequencies, as well as spontaneous emission rates characterizing fine and hyperfine atomic structures. Indeed, in the short time intervals which we consider, the number of spontaneously emitted particle is negligible and the systems are quasi-stable. These facts permits to improve the results obtained in previous works studying different systems [44-46]. We consider the structure of the atomic levels of ^{85}Rb, ^{87}Rb and ^{133}Cs which improves the detection of Unruh effect and permits very precise temperature measurements.

The structure of the paper is the following: in sect. **2** we diagonalize the effective Hamiltonian of mixed meson systems by means of a complete biorthonormal set of states; we compute the geometric phase for mixed mesons and we show their links with CPT and CP violations. A numerical analysis for B_s mesons is also presented. In sect. **3** we analyze the geometric phase for a two level atom undergoing a non-unitary evolution and study the possible applications to the detection of the Unruh effect and to build a very precise thermometer. Section **4** is devoted to the conclusions.

We are glad to dedicate this paper to Professor Gaetano Vilasi in the occasion of his 70th birthday.

2. – Meson mixing, CP and CPT violations and geometric phase

The particle mixing phenomenon has been analyzed thoroughly in the contexts of quantum mechanics (QM) [47-50] and of quantum field theory (QFT) [33-35, 51-55]. Although the QFT analysis discloses features which cannot be ignored (see for example refs. [34,53-56]), nevertheless a correct phenomenological description of systems as B^0-$\bar{B}^0$ can be also dealt with in the context of QM. Therefore, in the following we analyze the mixed bosons in the context of QM.

The state vector of mixed boson systems as K^0, B_d^0, B_s^0 and D^0 can be represented as $|\psi(t)\rangle = \psi_{M^0}(t)|M^0\rangle + \psi_{\bar{M}^0}(t)|\bar{M}^0\rangle + \sum_n d_n(t)|n\rangle$, where M^0 is the meson state (K^0, B_d^0, B_s^0 or D^0); $\bar{M}^0$ is the corresponding antiparticle, $|n\rangle$ are the decay products, t is the proper time, $\psi_{M^0}(t)$, $\psi_{\bar{M}^0}(t)$ and $d_n(t)$ are time dependent functions. At initial time $t = 0$ one has $|\psi(0)\rangle = \psi_{M^0}(0)|M^0\rangle + \psi_{\bar{M}^0}(0)|\bar{M}^0\rangle$. The time evolution of $|\psi(t)\rangle$ can be described, in the space formed by $|M^0\rangle$ and $|\bar{M}^0\rangle$ by means of the Schrödinger equation $i\frac{\mathrm{d}}{\mathrm{d}t}\Psi = \mathcal{H}\,\Psi$, where $\Psi = (\psi_{M^0}(t), \psi_{\bar{M}^0}(t))^T$ and $\mathcal{H}$ is the effective non-Hermitian

Hamiltonian of the system, $\mathcal{H} = \begin{pmatrix} \mathcal{H}_{11} & \mathcal{H}_{12} \\ \mathcal{H}_{21} & \mathcal{H}_{22} \end{pmatrix}$. Here $\mathcal{H} = M - i\frac{\Gamma}{2}$, with M and Γ Hermitian matrices. The matrix elements of $\mathcal{H}$ are constrained by the conservation of discrete symmetries [50]. Indeed, CPT conservation implies $\mathcal{H}_{11} = \mathcal{H}_{22}$, T conservation requires $|\mathcal{H}_{12}| = |\mathcal{H}_{21}|$ and CP conservation imposes $\mathcal{H}_{11} = \mathcal{H}_{22}$ and $|\mathcal{H}_{12}| = |\mathcal{H}_{21}|$.

In particular, the CP violation, (*i.e.* $|\mathcal{H}_{12}| \neq |\mathcal{H}_{21}|$), makes the Hamiltonian $\mathcal{H}$ non-Hermitian, $\mathcal{H} \neq \mathcal{H}^\dagger$ and non-normal, $[\mathcal{H}, \mathcal{H}^\dagger] \neq 0$ ([1]). Thus, the left and right eigenstates of $\mathcal{H}$ are independent sets of vectors that are not connected by complex conjugation, then the diagonalization of $\mathcal{H}$ needs the use of non-Hermitian quantum mechanics. We will use the biorthonormal basis formalism [57-59].

We denote with $\lambda_j = m_j - i\Gamma_j/2$, with $j = L, H$ (L denotes the light mass state and H the heavy mass state) the eigenvalues of the Hamiltonian $\mathcal{H}$ and with $|M_j\rangle$, the corresponding eigenvectors, $\mathcal{H}|M_j\rangle = \lambda_j|M_j\rangle$. Denoting with $|\widetilde{M_j}\rangle$, ($j = L, H$) the eigenvectors of $\mathcal{H}^\dagger$, the eigenvalues of $\mathcal{H}^\dagger$ are the complex conjugate of those of $\mathcal{H}$, $\mathcal{H}^\dagger|\widetilde{M_j}\rangle = \lambda_j^*|\widetilde{M_j}\rangle$. Notice that the conjugate states $\langle\widetilde{M_j}|^\dagger \equiv |\widetilde{M_j}\rangle$ and $|M_j\rangle^\dagger \equiv \langle M_j|$ are not isomorphic to their duals: $|\widetilde{M_j}\rangle \neq |M_j\rangle$ and $\langle M_j| \neq \langle\widetilde{M_j}|$. In this case, a complete biorthonormal set for $\mathcal{H}$ is given by $\{|M_j\rangle, \langle\widetilde{M_j}|\}$, with $j = L, H$. Indeed one has the following biorthogonality relation $\langle\widetilde{M_i}|M_j\rangle = \langle M_j|\widetilde{M_i}\rangle = \delta_{ij}$, and the completeness relations $\sum_j |M_j\rangle\langle\widetilde{M_j}| = \sum_j |\widetilde{M_j}\rangle\langle M_j| = 1$. The existence of a complete biorthonormal set of eigenvector of $\mathcal{H}$ implies that $\mathcal{H}$ is diagonalizable.

Moreover, since the time evolution operator associated with $\mathcal{H}$, $U(t) = e^{-i\mathcal{H}t}$ is not unitary, then we introduce the time evolution operator of $\mathcal{H}^\dagger$, $\widetilde{U}(t) = e^{-i\mathcal{H}^\dagger t}$, such that $U\widetilde{U}^\dagger = \widetilde{U}^\dagger U = 1$. The time evolved of the states $|M_k\rangle$ and $|\widetilde{M_k}\rangle$, ($k = L, H$) are thus $|M_k(t)\rangle = U(t)|M_k\rangle = e^{-i\lambda_k t}|M_k\rangle$ and $|\widetilde{M_k}(t)\rangle = \widetilde{U}(t)|\widetilde{M_k}\rangle = e^{-i\lambda_k^* t}|\widetilde{M_k}\rangle$.

By introducing the CP parameter $\varepsilon = \frac{|p/q|-|q/p|}{|p/q|+|q/p|} = \frac{|\mathcal{H}_{12}|-|\mathcal{H}_{21}|}{|\mathcal{H}_{12}|+|\mathcal{H}_{21}|}$, where $q/p = \sqrt{\mathcal{H}_{21}/\mathcal{H}_{12}}$, and the CPT parameter, $z = \frac{(\mathcal{H}_{22}-\mathcal{H}_{11})}{\lambda_L-\lambda_H}$, we derive the correct meson states $|M^0(t)\rangle$ and $|\bar{M}^0(t)\rangle$ in terms of the eigenstates of $\mathcal{H}$ $|M_L\rangle$ and $|M_H\rangle$ [41], which have to be used in the computations,

$$|M^0(t)\rangle = \frac{1}{2p}\left[\sqrt{1-z}\,|M_L\rangle\, e^{-i\lambda_L t} + \sqrt{1+z}\,|M_H\rangle\, e^{-i\lambda_H t}\right], \tag{1}$$

$$|\bar{M}^0(t)\rangle = \frac{1}{2q}\left[\sqrt{1+z}\,|M_L\rangle\, e^{-i\lambda_L t} - \sqrt{1-z}\,|M_H\rangle\, e^{-i\lambda_H t}\right], \tag{2}$$

$$\langle\widetilde{M^0}(t)| = p\,\left[\sqrt{1-z}\,\langle\widetilde{M_L}|\, e^{i\lambda_L t} + \sqrt{1+z}\,\langle\widetilde{M_H}|\, e^{i\lambda_H t}\right], \tag{3}$$

$$\langle\widetilde{\bar{M}^0}(t)| = q\,\left[\sqrt{1+z}\,\langle\widetilde{M_L}|\, e^{i\lambda_L t} - \sqrt{1-z}\,\langle\widetilde{M_H}|\, e^{i\lambda_H t}\right]. \tag{4}$$

We now study the geometric phase for mixed mesons. We consider the phase for pure states with a diagonalizable non-Hermitian Hamiltonian $\mathcal{H}_{NH}(t)$ [5] and analyze its extension to the biorthonormal basis formalism. In this case, the geometric phase is defined as [41] $\Phi_{NH}(t) = \arg\langle\widetilde{\psi}_{NH}(0)|\psi_{NH}(t)\rangle - \Im\int_0^t\langle\widetilde{\psi}_{NH}(t')|\dot{\psi}_{NH}(t')\rangle \mathrm{d}t'$, which is reparametrization invariant and it is invariant under the complex gauge transformations [41]. Here $|\psi_{NH}(t)\rangle$ and $|\widetilde{\psi}_{NH}(t)\rangle$ are the solution to the

([1]) The matrices M and Γ do not commute, $[M, \Gamma] \neq 0$.

Schrödinger equation $i(d/dt)|\psi_{NH}(t)\rangle = \mathcal{H}_{NH}(t)|\psi_{NH}(t)\rangle$ and to its adjoint equation $i(d/dt)|\widetilde{\psi}_{NH}(t)\rangle = \mathcal{H}^{\dagger}_{NH}(t)|\widetilde{\psi}_{NH}(t)\rangle$, respectively.

In the particular case of mixed meson systems $M^0 - \bar{M}^0$ one has the following phases [41]:

$$\Phi_{M^0M^0}(t) = \arg\langle\widetilde{M^0}(0)|M^0(t)\rangle - \Im\int_0^t \langle\widetilde{M^0}(t')|\dot{M}^0(t')\rangle \mathrm{d}t', \tag{5}$$

$$\Phi_{\bar{M}^0\bar{M}^0}(t) = \arg\langle\widetilde{\bar{M}^0}(0)|\bar{M}^0(t)\rangle - \Im\int_0^t \langle\widetilde{\bar{M}^0}(t')|\dot{\bar{M}}^0(t')\rangle \mathrm{d}t', \tag{6}$$

$$\Phi_{M^0\bar{M}^0}(t) = \arg\langle\widetilde{M^0}(0)|\bar{M}^0(t)\rangle - \Im\int_0^t \langle\widetilde{M^0}(t')|\dot{\bar{M}}^0(t')\rangle \mathrm{d}t', \tag{7}$$

$$\Phi_{\bar{M}^0M^0}(t) = \arg\langle\widetilde{\bar{M}^0}(0)|M^0(t)\rangle - \Im\int_0^t \langle\widetilde{\bar{M}^0}(t')|\dot{M}^0(t')\rangle \mathrm{d}t'. \tag{8}$$

$\Phi_{M^0M^0}(t)$ and $\Phi_{\bar{M}^0\bar{M}^0}(t)$ are the phases of the particle M^0 and of the antiparticle $\bar{M}^0$, respectively. They are connected to CPT violation parameter. $\Phi_{M^0\bar{M}^0}(t)$ and $\Phi_{\bar{M}^0M^0}(t)$ are the phases due to particle-antiparticle oscillations which are linked to CP violation (see below).

Denoting with $m = m_L + m_H$, $\Delta m = m_H - m_L$ and $\Delta\Gamma = \Gamma_H - \Gamma_L$, and assuming $\frac{\Delta\Gamma t}{2}$ small, which is valid in the range $|\Delta t| < 15\,\mathrm{ps}$ used in the experimental analysis on B^0-$\bar{B}^0$ system [60-62], eqs. (5) and (6) become

$$\Phi_{M^0M^0}(t) \simeq \arg\left[\cos\left(\frac{\Delta m t}{2}\right) + (\Im z - i\Re z)\sin\left(\frac{\Delta m t}{2}\right)\right] + \frac{t}{2}\left(\Delta m\,\Re z + \frac{\Delta\Gamma}{2}\,\Im z\right),$$

$$\Phi_{\bar{M}^0\bar{M}^0}(t) \simeq \arg\left[\cos\left(\frac{\Delta m t}{2}\right) - (\Im z - i\Re z)\sin\left(\frac{\Delta m t}{2}\right)\right] - \frac{t}{2}\left(\Delta m\,\Re z + \frac{\Delta\Gamma}{2}\,\Im z\right),$$

respectively (the explicit form of $\Phi_{M^0M^0}$ and $\Phi_{\bar{M}^0\bar{M}^0}$ for the general case are reported in ref. [41]). Notice that $\Phi_{M^0M^0}$ and $\Phi_{\bar{M}^0\bar{M}^0}$ depend on the real and imaginary part of the CPT parameter z and the difference phase, $\Delta\Phi(t) = \Phi_{M^0M^0}(t) - \Phi_{\bar{M}^0\bar{M}^0}(t)$ is due only to terms related to z. Indeed it is non-zero only in the presence of CPT violation. In the case of CPT invariance, $z = 0$, one has $\Phi^{CPT}_{M^0M^0}(t) = \Phi^{CPT}_{\bar{M}^0\bar{M}^0}(t) = \arg\left[\cos\left(\frac{\Delta m t}{2}\right)\right]$, which is trivially equal to 0 or π and $\Delta\Phi(t) = 0$.

On the other hand, the phases $\Phi_{M^0\bar{M}^0}(t)$ and $\Phi_{\bar{M}^0M^0}(t)$, for $\frac{\Delta\Gamma t}{2} \ll 1$ and omitting second order terms in z, (see ref. [41] for the general expressions) are

$$\Phi_{M^0\bar{M}^0}(t) \simeq \frac{\pi}{2} - \frac{mt}{2} + \arg\left[\frac{p}{q}\sin\left(\frac{\Delta m t}{2}\right)\right] - \frac{\Delta m t}{2}\,\Re\left(\frac{p}{q}\right) - \frac{\Delta\Gamma t}{2}\,\Im\left(\frac{p}{q}\right),$$

$$\Phi_{\bar{M}^0M^0}(t) \simeq \frac{\pi}{2} - \frac{mt}{2} + \arg\left[\frac{q}{p}\sin\left(\frac{\Delta m t}{2}\right)\right] - \frac{\Delta m t}{2}\,\Re\left(\frac{q}{p}\right) - \frac{\Delta\Gamma t}{2}\,\Im\left(\frac{q}{p}\right).$$

The phase difference is $\Phi_{M^0\bar{M}^0}(t) - \Phi_{\bar{M}^0M^0}(t) \neq 0$. On the contrary, in the case of CP conservation one has

$$\Phi^{CP}_{M^0\bar{M}^0}(t) = \Phi^{CP}_{\bar{M}^0M^0}(t) = \frac{\pi}{2} - (m + \Delta m)\frac{t}{2} + \arg\left[\sin\left(\frac{\Delta m t}{2}\right)\right], \tag{9}$$

and there is no phase difference.

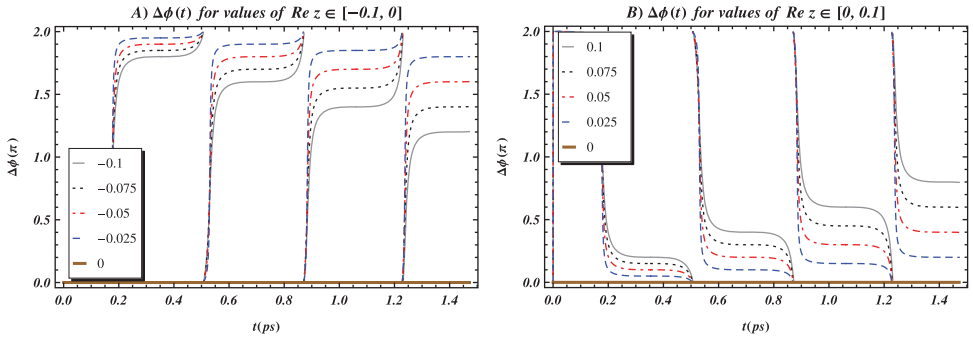

Fig. 1. – Plots of $\Delta\Phi = \Phi_{B_s^0 B_s^0} - \Phi_{\bar{B}_s^0 \bar{B}_s^0}$ as a function of time t for $\Im z = 0$ and different values of $\Re z$. In A) $\Delta\Phi(t)$ is reported for sample values of $\mathrm{Re} z \in [-0.1, 0]$ as indicated in the inset. In B) $\Delta\Phi(t)$ is plotted for sample values of $\mathrm{Re} z \in [0, 0.1]$ as shown in the inset.

Numerical analysis. – We present a numerical analysis of the phase related to z, $\Delta\Phi = \Phi_{M^0 M^0} - \Phi_{\bar{M}^0 \bar{M}^0}$ for the B_s system. Such a system is particulary appropriate for the study of non-cyclic phases since many particle oscillations occur within its lifetime. We use the following experimental data: $m_s = 1.63007 \times 10^{13}\,\mathrm{ps}^{-1}$, $\Delta m_s = 17.77\,\mathrm{ps}^{-1}$, $\Gamma_s = 0.678\,\mathrm{ps}^{-1}$, $\Delta\Gamma_s = -0.062\,\mathrm{ps}^{-1}$. Moreover, we assume, $-0.1 \leq \Re z \leq 0.1$ and $-0.1 \leq \Im z \leq 0.1$ [62]. Notice that, in such intervals for $\Re z$ and $\Im z$, the phase $\Delta\Phi$ is weakly depending on the value of $\Im z$, so that one can fix an arbitrary value of $\Im z$ in the values interval $[-0.1, 0.1]$ and study the non-cyclic phases as functions of time for different values of $\Re z$. In fig. 1, the phase is drawn for $\Im z = 0$. In order to better show the behavior of the phases, the figures contain two plots A) and B) of the same phase for sample values of $\Re z$ belonging to the intervals $[-0.1, 0]$ and $[0, 0.1]$, respectively. A non-zero phase difference $\Delta\Phi$ appears in the case of CPT violation.

3. – Unruh effect, quantum thermometer and geometric phase

In refs. [30, 31] we have shown that the phenomena characterized by the presence of vacuum condensate [36-40] are also characterized by the presence of Aharonov-Anandan invariant and of geometric phase. Thus the geometric phase can used to study the properties of such systems and to reveal phenomena like Unruh, Casimir effects, or quantum field theory (QFT) in curved background, which are elusive to the observations.

Here we focus our attention on the Unruh effect and on the possibility of the realization of a quantum thermometer. To do that we consider quantum open systems and use the Wang and Liu approach [16] to define the geometric phase for mixed states in nonunitary, noncyclic evolution.

Geometric phase for mixed states in nonunitary, noncyclic evolution. – The geometric phase is defined as

$$\Phi_g = \sum_{k=1}^{N} \arg\left[\sqrt{\lambda_k(t_0)\lambda_k(t)}\,\langle\varphi_k(t_0)|\varphi_k(t)\rangle\right] - \Im\sum_{k=1}^{N}\int_{t_0}^{t}\lambda_k(t')\langle\varphi_k(t')|\frac{\partial}{\partial t'}|\varphi_k(t')\rangle \mathrm{d}t', \tag{10}$$

where $|\varphi_k(t)\rangle$ and $\lambda_k(t)$ are eigenstates and eigenvalues of the matrix density $\rho(t)$ describing the quantum open system for N-level mixed states. The first term of eq. (10) represents the total phase, the second term the dynamic one.

In the case of a two level open system, $N = 2$, the radius of Block sphere is $r(t) = \sqrt{n_1^2 + n_2^2 + n_3^2}$, with $n_1 = \rho_{12} + \rho_{21}$, $n_2 = i(\rho_{12} - \rho_{21})$, $n_3 = \rho_{11} - \rho_{22}$. Defining the angles $\theta = \cos^{-1}(n_3/r)$ and $\phi = \tan(n_2/n_1)$, the eigenvectors of ρ, $|\varphi_1(t)\rangle$ and $|\varphi_2(t)\rangle$ are (apart overall phase factors)

$$|\varphi_1(t)\rangle = \begin{pmatrix} \cos\dfrac{\theta(t)}{2} \\ e^{i\phi(t)}\sin\dfrac{\theta(t)}{2} \end{pmatrix}, \qquad |\varphi_2(t)\rangle = \begin{pmatrix} \sin\dfrac{\theta(t)}{2} \\ -e^{i\phi(t)}\cos\dfrac{\theta(t)}{2} \end{pmatrix},$$

and the eigenvalues are $\lambda_1(t) = \frac{1}{2}[1 + r(t)]$ and $\lambda_2 = \frac{1}{2}[1 - r(t)]$.

Interaction. – Let us now consider the Hamiltonian [63], $H = \frac{\hbar}{2}\omega_0\,\sigma_3 + H_F - \sum_{mn}\mu_{mn}\cdot\mathbf{E}(x(t))\sigma_{mn}$, which describes a two level atom as an open system with a non-unitary evolution in the reservoir of the electromagnetic field. In H, ω_0 is the energy level spacing of the atom, σ_3 is the Pauli matrix, H_F is the electromagnetic field Hamiltonian, μ_{mn} is the matrix element of the dipole momentum operator connecting single-particle states u_n and $u_{n'}$ ([63]), $\sigma_{mn} = \sigma_m\sigma_n$, and $\mathbf{E}$ is the strength of the electric field. We consider a weak interaction between atom and field and study the evolution of the total density matrix $\rho_{\rm tot} = \rho(0)\otimes|0\rangle\langle 0|$, in the frame of the atom. Here $|0\rangle$ and $\rho(0)$ are the vacuum and the initial reduced density matrix of the atom. The evolution is given by [64, 65]

$$\frac{\partial\rho(\tau)}{\partial\tau} = -\frac{i}{\hbar}[H_{\rm eff},\rho(\tau)] + \frac{1}{2}\sum_{i,j=1}^{3} a_{ij}\left(2\sigma_j\,\rho\,\sigma_i - \sigma_i\,\sigma_j\,\rho - \rho\,\sigma_i\,\sigma_j\right), \tag{11}$$

with τ proper time, $H_{\rm eff}$ effective hamiltonian, $H_{\rm eff} \simeq \frac{\hbar}{2}\omega_0\,\sigma_3$, ($\omega_0$ is the atomic transition frequency, we neglect the Lamb shift terms), a_{ij} coefficients of the Kossakowski matrix, $a_{ij} = \Sigma\,\delta_{ij} - i\Upsilon\,\epsilon_{ijk}\delta_{k3} - \Sigma\,\delta_{i3}\delta_{j3}$, with $\Sigma = \frac{1}{4}[G(\omega_0) + G(-\omega_0)]$, $\Upsilon = \frac{1}{4}[G(\omega_0) - G(-\omega_0)]$, and $G(\omega) = \int_{-\infty}^{\infty}{\rm d}\tau e^{i\omega\tau}G^+(x(\tau))$ Fourier transform of $G^+(x-y) = \frac{e^2}{\hbar^2}\sum_{i,j=1}^{3}\langle +|r_i|-\rangle\langle -|r_j|+\rangle\langle 0|E_i(x)E_j(x)|0\rangle$.

For an initial state of the atom given by $|\psi(0)\rangle = \cos\left(\frac{\theta}{2}\right)|+\rangle + \sin\left(\frac{\theta}{2}\right)|-\rangle$, with $\theta \equiv \theta(0)$, one has the reduced density matrix $\rho(\tau)$ [30, 31, 45]

$$\rho(\tau) = \frac{1}{2}\begin{pmatrix} \chi+1 & e^{-i\Omega\tau}\sqrt{\xi^2-\chi^2} \\ e^{i\Omega\tau}\sqrt{\xi^2-\chi^2} & 1-\chi \end{pmatrix}, \tag{12}$$

where $\xi(\tau) = \sqrt{\chi^2 + e^{-4\Sigma\tau}\sin^2\theta}$, and $\chi(\tau) = e^{-4\Sigma\tau}\cos\theta + \frac{\Upsilon}{\Sigma}(e^{-4\Sigma\tau} - 1)$.

The eigenvalues and the corresponding eigenvectors of $\rho(\tau)$ are: $\lambda_\pm = \frac{1}{2}(1 \pm \xi)$, and

$$\begin{aligned} |\phi_+(\tau)\rangle &= \cos\left(\frac{\theta(\tau)}{2}\right)|+\rangle + \sin\left(\frac{\theta(\tau)}{2}\right)e^{i\Omega\tau}|-\rangle, \\ |\phi_-(\tau)\rangle &= \sin\left(\frac{\theta(\tau)}{2}\right)|+\rangle - \cos\left(\frac{\theta(\tau)}{2}\right)e^{i\Omega\tau}|-\rangle. \end{aligned} \tag{13}$$

Considering the initial time $t_0 = 0$, the geometric phase (10) becomes

$$\Phi_g(t) = \arg\left[\cos\frac{\theta}{2}\cos\frac{\theta(t)}{2} + \sin\frac{\theta}{2}\sin\frac{\theta(t)}{2}e^{i\Omega t}\right] - \frac{\Omega}{2}\int_0^t [1 - \xi(\tau)\cos\theta(\tau)]\,\mathrm{d}\tau, \tag{14}$$

with $\theta \equiv \theta(0)$. Such a phase can be used in the detection of Unruh effect and in the building of a quantum thermometer.

Unruh effect. – In the case of Unruh effect, we study the difference between two geometric phase (14) computed for the two level system in the presence of an acceleration and in the inertial case. Such a phase difference is due only to the atom acceleration and then to the Unruh effect, since the accelerated system sees the Minkowski vacuum as a thermal Rindler vacuum.

Considering the atom acceleration through Minkowski spacetime in the x direction, the Rindler coordinates are $x(\tau) = \frac{c^2}{a}\cosh\frac{a\tau}{c}$, $t(\tau) = \frac{c}{a}\sinh\frac{a\tau}{c}$. Then the function $\sin\frac{\theta(t)}{2} = \pm\sqrt{\frac{1}{2}\left(1 - \frac{\chi(t)}{\xi(t)}\right)}$ in eq. (14) becomes

$$\sin\frac{\theta_a(t)}{2} = \pm\sqrt{\frac{1}{2} - \frac{R_a - R_a\,e^{4\Sigma_a t} + \cos\theta}{2\sqrt{e^{4\Sigma_a t}\sin^2\theta + \left(R_a - R_a\,e^{4\Sigma_a t} + \cos\theta\right)^2}}}, \tag{15}$$

and similar for $\cos\frac{\theta_a(t)}{2}$, where $R_a = \Upsilon_a/\Sigma_a$, with $\Sigma_a = \frac{\gamma_0}{4}\left(1 + \frac{a^2}{c^2\omega_0^2}\right)\frac{e^{2\pi c\omega_0/a}+1}{e^{2\pi c\omega_0/a}-1}$ and $\Upsilon_a = \frac{\gamma_0}{4}\left(1 + \frac{a^2}{c^2\omega_0^2}\right)$, and γ_0 spontaneous emission rate.

Equation (14) holds also for an inertial atom, $a = 0$. In this case, $\sin\frac{\theta_a(t)}{2}$, $\cos\frac{\theta_a(t)}{2}$ and $\cos\theta_a(t)$ are replaced by $\sin\frac{\theta_{a=0}(t)}{2}$, $\cos\frac{\theta_{a=0}(t)}{2}$ and $\cos\theta_{a=0}(t)$ in which Σ_a, Υ_a, R_a are replaced by $\Sigma_{a=0} = \Upsilon_{a=0} = \gamma_0/4$, $R_{a=0} = 1$.

The phase difference $\Delta\Phi_U(t) = \Phi_a(t) - \Phi_{a=0}(t)$, gives the geometric phase in terms of the acceleration a.

Notice that the atomic element which has to be used in the interferometer plays an important role, since a non trivial value of $\Delta\Phi_U(t)$ can be achieved when $\gamma_0/\omega_0 > 10^{-5}$.

In fig. 2 we plot $\Delta\Phi_U$ as function of the acceleration a for different hyperfine level structures of ^{85}Rb, ^{87}Rb and ^{133}Cs, as reported in the caption of the picture.

Values of $\Delta\Phi_U \sim 10^{-4}\pi$, which are accessible with the current technology, can be obtained for accelerations of order of $10^{16}\,\mathrm{m/s^2}$ and speeds of order of (0.2–0.3)c. The time intervals considered are of order of $1/\omega_0$ in order to have negligible spontaneous emission ($N(t \sim 1/\omega_0) \sim 0.98N(0)$). The geometric phase above described can be revealed with a Mach-Zehnder interferometer with branches of length of 4 cm. In particular, a difference in the arm lengths of the interferometer of about 0.1 μm permits to remove almost completely the dynamical phase differences δ and to reveal only the geometric phase [31].

Quantum thermometer. – The geometric phase of eq. (14) appears also when an atom interacts with thermal states. Therefore, its analysis could allow very precise measurement of the temperature.

In the case of thermal states, the above coefficients Υ_a and Σ_a are replaced by Σ_T and Υ_T which depend on the temperature [30, 31], $\Upsilon_T = (\gamma_0/4)\,(1 + 4\pi^2 k_B^2 T^2/\hbar^2\omega_0^2)$, and $\Sigma_T = (\gamma_0/4)\,(1 + 4\pi^2 k_B^2 T^2/\hbar^2\omega_0^2)\,(e^{E_0/k_B T} + 1)/(e^{E_0/k_B T} - 1)$, $E_0 = \hbar\omega_0$.

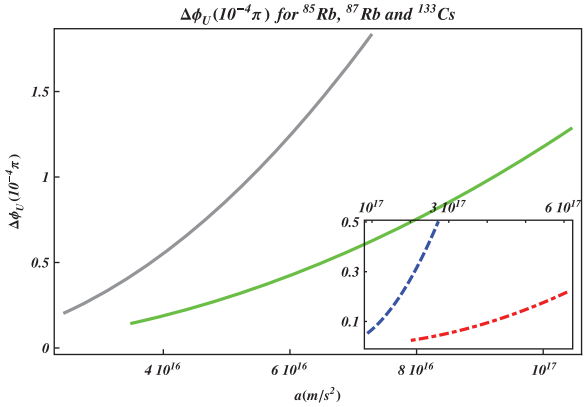

Fig. 2. – Plots of $\Delta\Phi_U$ as a function of the atom acceleration a, for time intervals $t \simeq 1/\omega_0$ and the splitting between the hyperfine energy levels: main pictures: (gray) dot dashed line: ^{87}Rb, $5^2P_{1/2}$ line, splitting for $F = 1 \to F = 2$ transition ($\omega_0 = 814.5\,\text{MHz}$, $\gamma_0 = 36.129\,\text{MHz}$ [66]); (green) solid line: ^{133}Cs, $6^2P_{1/2}$ line, splitting of the between the $F = 3$ and $F = 4$ levels ($\omega_0 = 1167.68\,\text{MHz}$, $\gamma_0 = 28.743\,\text{MHz}$ [67]). Pictures in the inset: (blue) dashed line: ^{85}Rb, $5^2S_{1/2}$ line, energy splitting between the levels $F = 1$ and $F = 2$ ($\omega_0 = 3.035\,\text{GHz}$, $\gamma_0 = 36.129\,\text{MHz}$ for D_1 transition, $\gamma_0 = 38.117\,\text{MHz}$ for D_2 transition [68]); (red) dot dashed line: ^{87}Rb, $5^2S_{1/2}$ line, energy splitting between the levels $F = 1$ and $F = 2$ ($\omega_0 = 6.843\,\text{GHz}$, $\gamma_0 = 36.129\,\text{MHz}$ for D_1 transition, $\gamma_0 = 38.117\,\text{MHz}$ for D_2 transition [66]).

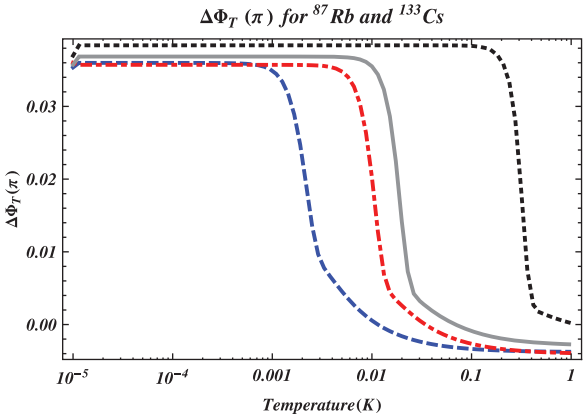

Fig. 3. – Plots of $\Delta\Phi_T$ as function of the temperatures of cold sources T_c, for the splitting between the hyperfine energy levels and T_h values: (blue) dashed line: ^{133}Cs, $6^2P_{3/2}$ line, splitting for $F = 4 \to F = 5$ transition ($\omega_0 = 251.09\,\text{MHz}$, $\gamma_0 = 32.889\,\text{MHz}$ [67]) and $T_h = 10^{-2}\,\text{K}$; (red)dot-dashed line: ^{87}Rb, $5^2P_{1/2}$ line, splitting for $F = 1 \to F = 2$ transition ($\omega_0 = 814.5\,\text{MHz}$, $\gamma_0 = 36.129\,\text{MHz}$ [66]), and $T_h = 3 \times 10^{-2}\,\text{K}$; (gray) solid line: ^{133}Cs, $6^2P_{1/2}$ line, splitting for $F = 3 \to F = 4$ transition ($\omega_0 = 1167.68\,\text{MHz}$, $\gamma_0 = 28.743\,\text{MHz}$ [67]) and $T_h = 6 \times 10^{-2}\,\text{K}$; (black) dotted line: ^{133}Cs, $6^2S_{1/2}$ line, splitting for $F = 3 \to F = 4$ transition ($\omega_0 = 9.192\,\text{GHz}$, $\gamma_0 = 28.743\,\text{MHz}$ [67]) and $T_h = 1\,\text{K}$. The time considered is $t \simeq \frac{1}{4\omega_0}\,\text{s}$.

Then a quantum thermometer can be built by means of an interferometer in which an atom follows two different paths interacting with two thermal states at different temperatures. Assuming known the temperature of one thermal state, the temperature of

the other one can be obtained by measuring the difference between the geometric phases generated in the two paths. In the following we assume known the temperature T_h of the hotter source and we derive the temperature T_c of the colder source by measuring $\Delta\Phi_T$.

Also in this case we consider the hyperfine structure of ^{133}Cs, and ^{87}Rb and we plot in fig. 3, $\Delta\Phi_T$ as function of the temperatures of cold sources T_c, for different lines and different values of T_h. We consider time intervals $t \simeq \frac{1}{4\omega_0}$ s in order that the particle decay can be neglected and we obtain temperatures of the cold source of ~ 2 orders of magnitude below the reference temperature of the hot source. Paths of slightly different lengths can be chosen in order to let the geometric phase be dominating over the relative dynamical phase.

4. – Conclusions

We have studied the geometric phase for different phenomena and analyzed its possible applications. We have shown that the geometric phases generated by the evolution of mixed meson systems depend on the CPT violating parameter z [41]. In particular, we have shown that a nonzero difference of phase $\Delta\Phi$ between particle and antiparticle appears only in the case of CPT symmetry breaking. Therefore, in the next future, accurate analysis of the geometric phases for mixed mesons like the neutral B_s system and the kaons, might represent a completely alternative method to test one of the most important symmetries of the nature. The geometric phase can allow also the study of the CP symmetry breaking in mixed mesons.

Moreover, we have analyzed the geometric phase for mixed state with a non-unitary evolution and we have shown that the geometric phase of atoms accelerated in an interferometer could permit the laboratory detection of the Unruh effect. Similar atoms, interacting with two different thermal states can be utilized in an interferometer to have very precise temperature measurements [31].

* * *

Partial financial support from MIUR and INFN is acknowledged.

REFERENCES

[1] Berry M. V., *Proc. R. Soc. Lond. A*, **392** (1984) 45.
[2] Aharonov Y. and Anandan J., *Phys. Rev. Lett.*, **58** (1987) 1593.
[3] Samuel J. and Bhandari R., *Phys. Rev. Lett.*, **60** (1988) 2339.
[4] Anandan J. and Aharonov Y., *Phys. Rev. Lett.*, **65** (1990) 1697.
[5] Mukunda N. and Simon R., *Ann. Phys. (N.Y)*, **228** (1993) 205.
[6] Garcia de Polavieja G., *Phys. Rev. Lett.*, **81** (1998) 1.
[7] Pancharatnam S., *Proc. Indian Acad. Sci. A*, **44** (1956) 1225.
[8] Shapere A. and Wilczek F., *Geometric Phases in Physics* (World Scientific, Singapore) 1989.
[9] Simon B., *Phys. Rev. Lett.*, **51** (1983) 2167.
[10] Garrison J. C. and Wright E. M., *Phys. Lett. A*, **128** (1988) 177.
[11] Garrison J. C. and Chiao R. Y., *Phys. Rev. Lett.*, **60** (1988) 165.
[12] Pati A. K., *J. Phys. A*, **28** (1995) 2087.
[13] Pati A. K., *Phys. Rev. A*, **52** (1995) 2576.
[14] Anandan J., *Phys. Lett. A*, **133** (1988) 171.
[15] Mostafazadeh A., *J. Phys. A*, **32** (1999) 8157.
[16] Wang Z. S. and Liu Q., *Phys. Lett. A*, **377** (2013) 3272.

[17] Uhlmann A., *Rep. Math. Phys.*, **24** (1986) 229.
[18] Sjqvist E. *et al.*, *Phys. Rev. Lett.*, **85** (2000) 2845.
[19] Carollo A., Fuentes-Guridi I., Santos M. F. and Vedral V., *Phys. Rev. Lett.*, **90** (2003) 160402.
[20] Wang Z. S., Kwek L. C., Lai C. H. and Oh C. H., *Europhys. Lett.*, **74** (2006) 958.
[21] Chaturvedi S., Ercolessi E., Marmo G., Morandi G., Mukunda N. and Simon R., *Eur. Phys. J. C*, **35** (2004) 413.
[22] Ericsson M., Pati A. K., Sjqvist E., Brnnlund J. and Oi D. K. L., *Phys. Rev. Lett.*, **91** (2003) 090405.
[23] Tong D. M., Sjoqvist E., Kwek L. C. and Oh C. H., *Phys. Rev. Lett.*, **93** (2004) 080405.
[24] Bruno A., Capolupo A., Kak S., Raimondo G. and Vitiello G., *Mod. Phys. Lett. B*, **25** (2011) 1661.
[25] Tomita A. and Chiao R. Y., *Phys. Rev. Lett.*, **57** (1986) 937.
[26] Jones J. A., Vedral V., Ekert A. and Castagnoli G., *Nature*, **403** (2000) 869.
[27] Leek P. J. *et al.*, *Science*, **318** (2007) 1889.
[28] Neeley M. *et al.*, *Science*, **325** (2009) 722.
[29] Pechal M. *et al.*, *Phys. Rev. Lett.*, **108** (2012) 170401.
[30] Capolupo A. and Vitiello G., *Phys. Rev. D*, **88** (2013) 024027.
[31] Capolupo A. and Vitiello G., *Adv. High Energy Phys.*, **2015** (2015) 878043.
[32] Umezawa H., *Advanced field theory: Micro, macro, and thermal physics* (AIP, New York) 1993.
[33] Blasone M., Capolupo A., Romei O. and Vitiello G., *Phys. Rev. D*, **63** (2001) 125015.
[34] Capolupo A., Ji C. R., Mishchenko Y. and Vitiello G., *Phys. Lett. B*, **594** (2004) 135.
[35] Blasone M., Capolupo A. and Vitiello G., *Phys. Rev. D*, **66** (2002) 025033 and references therein.
[36] Unruh W. G., *Phys. Rev. D*, **14** (1976) 870.
[37] Hawking S. W., *Commun. Math. Phys.*, **43** (1975) 199 (Erratum-ibid. **46** (1976) 206).
[38] Parker L., *Phys. Rev. Lett.*, **21** (1968) 562.
[39] Schrödinger E., *Physica*, **6** (1939) 899.
[40] Birrell N. D. and Davies P. C. W., *Quantum Fields in Curved Space Cambridge Mono. Math. Phys.* (Cambridge University Press) 1984.
[41] Capolupo A., *Phys. Rev. D*, **84** (2011) 116002.
[42] Capolupo A., Lambiase G. and Vitiello G., *Adv. High. Energy Phys.*, **2015** (2015) 826051.
[43] Capolupo A. and Vitiello G., *Adv. High Energy Phys.*, **2013** (2013) 850395.
[44] Martin-Martinez E., Fuentes I. and Mann R. B., *Phys. Rev. Lett.*, **107** (2011) 131301.
[45] Hu J. and Yu H., *Phys. Rev. A*, **85** (2012) 032105.
[46] Martin-Martinez E., Dragan E. A., Mann R. B. and Fuentes I., *New J. Phys.*, **69** (2013) 053036.
[47] Kabir P. K., *The CP Puzzle* (Academic Press, London) 1968; Nachtmann O., *Elementary Particle Physics: Concepts and Phenomena* (Springer, Berlin) 1990.
[48] Bilenky S. M. and Pontecorvo B., *Phys. Rep.*, **41** (1978) 225.
[49] Lenz A. and Nierste U., *J. High Energy Phys.*, **06** (2007) 072.
[50] Fidecaro M. and Gerber H. J., *Rep. Prog. Phys.*, **69** (2006) 1713 (Erratum **69** (2006) 2841) and references therein.
[51] Blasone M., Capolupo A., Terranova F. and Vitiello G., *Phys. Rev. D*, **72** (2005) 013003.
[52] Blasone M., Capolupo A., Ji C.-R. and Vitiello G., *Int. J. Mod. Phys. A*, **25** (2010) 4179.

[53] Capolupo A., Capozziello S. and Vitiello G., *Phys. Lett. A*, **363** (2007) 53; *Int. J. Mod. Phys. A*, **23** (2008) 4979; Blasone M., Capolupo A., Capozziello S. and Vitiello G., *Nucl. Instrum. Meth. A*, **588** (2008) 272; Blasone M., Capolupo A. and Vitiello G., *Prog. Part. Nucl. Phys.*, **64** (2010) 451; Blasone M., Capolupo A., Capozziello S., Carloni S. and Vitiello G., *Phys. Lett. A*, **323** (2004) 182.
[54] Capolupo A., Capozziello S. and Vitiello G., *Phys. Lett. A*, **373** (2009) 601.
[55] Capolupo A., Di Mauro M. and Iorio A., *Phys. Lett. A*, **375** (2011) 3415.
[56] Capolupo A. and Di Mauro M., *Phys. Lett. A*, **376** (2012) 2830; *Acta Phys. Polon. B*, **44** (2013) 81; Vacuum condensates as a mechanism of spontaneous supersymmetry breaking, *Adv. High Energy Phys.*, in press.
[57] Bender C. M. and Boettcher S., *Phys. Rev. Lett.*, **80** (1998) 5243; Tanaka T., *J. Phys. A: Math. Gen.*, **39** (2006) 7757.
[58] Baker H. C. and Singleton jr. R. L., *Phys. Rev. A*, **42** (1990) 10.
[59] Dattoli G., Torre A. and Mignani R., *Phys. Rev. A*, **42** (1990) 1467.
[60] Aubert B. *et al.* [BABAR Collaboration], *Phys. Rev. D*, **70** (2004) 012007.
[61] Aubert B. *et al.* [BABAR Collaboration], *Phys. Rev. Lett.*, **96** (2006) 251802.
[62] Aubert B. *et al.* [BABAR Collaboration], *Phys. Rev. Lett.*, **100** (2008) 131802.
[63] Compagno G., Passante R. and Persico F., *Atom-field interactions and dressed atoms* (Cambridge University Press, Cambridge) 1995.
[64] Lindblad G., *Commun. Math. Phys.*, **48** (1976) 119.
[65] Gorini V., Kossakowski A. and Sudarshan E. C., *J. Math. Phys.*, **17** (1976) 821.
[66] Steck D. A., Rubidium 87 D Line Data, available online at `http://steck.us/alkalidata` (revision 2.1.4, 23 December 2010).
[67] Steck D. A., Cesium D Line Data, available online at `http://steck.us/alkalidata` (revision 2.1.4, 23 December 2010).
[68] Steck D. A., Rubidium 85 D Line Data, available online at `http://steck.us/alkalidata` (revision 2.1.6, 20 September 2013).